

# An Investigation of Haptic Perception of Viscoelastic Materials in the Frequency Domain

Ozan Caldiran<sup>1,\*</sup>, and Hong Z. Tan<sup>2</sup>, and Cagatay Basdogan<sup>1</sup>

**Abstract**—Although we hardly interact with objects that are purely elastic or viscous, haptic perception studies of deformable objects are mostly limited to stiffness and damping. Psychophysical investigation of materials that show both elastic and viscous behavior (viscoelastic materials) is challenging due to their complex, time and rate dependent mechanical behavior. In this study, we provide a new insight into the investigation of human perception of viscoelasticity in the frequency domain. In the frequency domain, the force response of a viscoelastic material can be represented by its magnitude and phase angle. Using this framework, we estimated the point of subjective equality (PSE) of a Maxwell arm (a damper and a spring in series) to a damper and a spring using complex stiffness magnitude and phase angle in two sets of experiments. A damper and a spring are chosen for the comparisons since they actually represent the limit cases for a viscoelastic material. We first performed 2I-2AFC adaptive staircase experiments to investigate how the perceived magnitude of complex stiffness changes in a Maxwell arm for small and large values of time constant. Then, we performed 3I-2AFC adaptive staircase experiments to investigate how the PSE changes as a function of the phase angle in a Maxwell arm. The results of our study show that the magnitude of complex stiffness was underestimated due to the smaller phase lag (with respect to a damper's) between the sinusoidal displacement applied by the participants to the Maxwell arm and the force felt in their finger when the time constant was small, whereas no difference was observed for a large time constant. Moreover, we observed that the PSE values estimated for the lower bound of the phase angle were significantly closer to their actual limit ( $0^\circ$ ) than those of the upper bound to  $90^\circ$ .

## I. INTRODUCTION

In daily life, we come into contact with different types of objects varying in their material properties. One such property is viscoelasticity. For example, when physicians and surgeons palpate soft tissues, accurate assessment of viscoelasticity is of the critical value for the correct diagnosis [1], or as in food and cosmetic industry, viscoelasticity might be an important indicator of product quality [2]. Nevertheless, our knowledge of haptic perception of viscoelastic materials is very limited.

On the other hand, haptic perception of compliance (reciprocal of stiffness) and viscosity, both of which can be

\*Ozan Caldiran is funded by the BIDEB-2211 Student Fellowship Program of The Scientific and Technological Research Council of Turkey (TUBITAK).

<sup>1</sup>Ozan Caldiran and Cagatay Basdogan are with the College of Engineering, Koc University, 34450 Istanbul, Turkey ocaldiran13@ku.edu.tr, cbasdogan@ku.edu.tr

<sup>2</sup>Hong Z. Tan is with the School of Electrical and Computer Engineering, Purdue University, West Lafayette, IN 47907, USA hongtan@purdue.edu

TABLE I  
JND OF HAPTIC RELATED QUANTITIES

	Signal detection	Contralateral limb matching
Position	1 to 3% [3]	8% [4]
Force	7% [5]	15% [6]
Stiffness (Compliance)	22% [7] (roving displacement)	23% [8]
Viscosity	14% [9]	34% [10]
Mass	21% [9]	

regarded as special cases of viscoelasticity have been thoroughly investigated not only for just-noticeable differences (JND) (see Table I), but also for the effect of numerous factors like time delay in force feedback ([11], [12], [13]), exploration strategies ([14], [15]), tool use ([14], [16], [17]), different cues used for discrimination ([14], [16], [18]), masking [19], and force direction [20]. On the other hand, even if we ignore the effect of the above factors, designing the most fundamental psychophysical experiments to investigate human haptic perception of viscoelastic materials is highly challenging due to their complex mechanical behavior. Mechanical response of viscoelastic materials depends on loading frequency and history, and a phase difference exists between force and input displacement or vice versa. Moreover, the force (displacement) response to displacement (force) input can be governed by multiple time-constants, as in the case of soft organ tissues [21], [22], [23], [24]. Hence, viscoelastic material models incorporate multiple parameters to account for this complex mechanical response unlike the simple spring and damper models utilized in most of the earlier studies on haptic perception of stiffness and viscosity.

To our knowledge, no general methodology has been proposed in the literature to investigate the haptic perception of viscoelasticity yet. In fact, only a few studies focused on the haptic perception of viscoelasticity. Nicholson et al. [1] questioned whether palpation is a reliable diagnostic tool to examine pathologies of human spine by conducting psychophysical experiments to investigate the capability of humans in manual discrimination of viscoelastic stimuli in the presence of kinesthetic cues. Nevertheless, they used a Kelvin-Voigt, which does not display the true relaxation/creep characteristics of soft organ tissues (see Fig. 1). Furthermore, only the stiffness component of the model was used in the analysis of the experimental data. On the other hand, in some other studies, rubber stimulus, which is also known to show viscoelastic behavior, is used for psychophys-

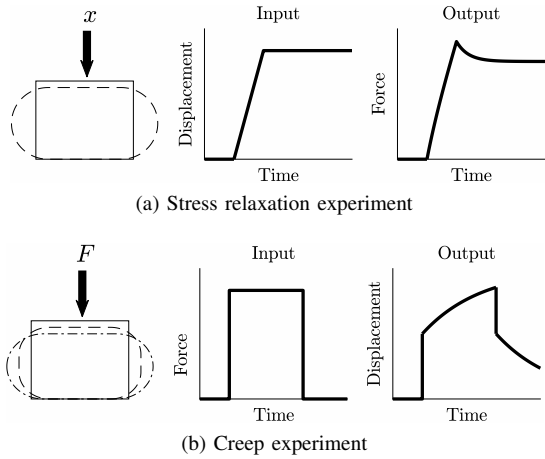


Fig. 1. Mechanical behavior of viscoelastic material

ical investigation of softness or compliance without a full material characterization of the samples [14], [16], [18]. However, it is well-known that viscoelastic materials are neither solely elastic nor viscous, but a mixture of both, thus resulting in a complex time-dependent behavior under even simple loading conditions. Only [16] used a single Maxwell arm (a spring and damper in series) for the characterization of their rubber stimuli, but, perhaps due to the complexity of the analysis, only the stiffness component of the model was again considered again for interpreting the results of their psychophysical experiments.

Studies focused on the effect of delay on perception of stiffness are also of particular relevance to this study since viscoelastic materials show a phase difference between force and displacement under dynamic loading. In [11], it was shown that stiffness is underestimated when force is leading the displacement, and overestimated when force is delayed. Later in [12], several cues were proposed as possible candidates to explain this shift in perception. Among them, the ratio of peak force to penetration depth was found to be the most likely candidate. The study was further extended in [25] to model the motor control under delay, and the authors defined motormetric curves analogous to psychometric curves. In [26], these motormetrics were used to assess the discrepancies between perception and action during a teleoperated needle insertion task, where soft tissue interactions were modeled by a nonlinear rigid boundary under delay. On the other hand, in [13], Rank et al. investigated the effect of delay on stiffness, damping, and inertia in the frequency domain. During the experiments, the participants were asked to make sinusoidal movements while interacting with the virtual force fields displaying the impedance characteristics of those three environments. For each virtual environment, the authors conducted an odd-one-out experiment, where the task was to identify the odd stimulus which was displayed with a delay. For all three types of impedances, the authors fitted psychometric curves to the discrimination performance of participants as a function of delay.

In this study, we present a novel approach for investigating

human haptic perception of viscoelasticity. We investigate human haptic perception of viscoelasticity in the frequency domain rather than in time domain. In the frequency domain, the response of a viscoelastic material can be simply characterized in terms of complex stiffness  $k_C(\omega)$ , which has real and imaginary components as shown below

$$k_C(\omega) = k_S(\omega) + j k_L(\omega) \quad (1)$$

where  $\omega$  is the frequency of stimulation. The real and imaginary components  $k_S$  and  $k_L$  are related to the energy storage and loss characteristics of the material and the ratio of  $k_L/k_S$  is known as the loss factor,  $\eta(\omega)$ . The above relation can also be written in terms of the magnitude of the complex stiffness and the phase angle,

$$k_C(\omega) = |k_C| \angle \phi \quad (2)$$

where  $\phi = \tan^{-1}(k_L/k_S)$  is the phase angle.

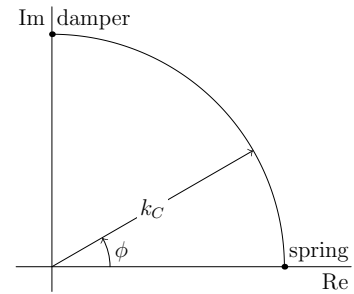


Fig. 2. Complex stiffness

We utilized these two parameters (magnitude and phase angle of the complex stiffness) to investigate human haptic perception of viscoelastic materials. As depicted in Fig. 2, we can view a spring (damper) as the limit case of a viscoelastic material with a complex stiffness that is purely real (imaginary). So, in our experiments, we determined the points of subjective equality (PSE) of a Maxwell arm corresponding to these special cases in terms of perceived magnitude (see Section III), as well as the upper and lower bounds of phase angle (see Section IV).

Before going into the details of our psychophysical experiments, we elaborate more on the mechanical behavior of a Maxwell arm under dynamic loading in the next section.

## II. MAXWELL ARM IN THE FREQUENCY DOMAIN

Generalized Maxwell Model (GMM) (see Fig. 3) is a proper viscoelastic model which can capture time and rate dependency of viscoelastic materials. One of the foundational units of a GMM is a Maxwell arm: a spring and a damper in series. Each Maxwell arm of a GMM represents a different time constant  $\tau$  of the modeled material. In this section, we investigate the mechanical response of a Maxwell arm with a large or a small time constant, i.e. the complex stiffness is close to being purely real or imaginary.

The governing equation of a Maxwell arm is given as

$$\frac{\dot{F}}{k_1} + \frac{F}{b_1} = \dot{x} \quad (3)$$

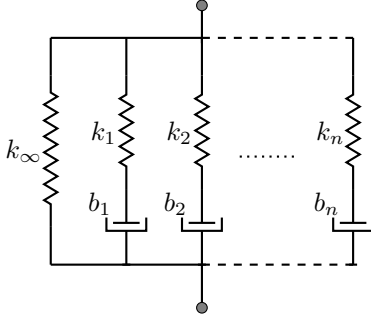


Fig. 3. Generalized Maxwell Model with  $n$  arms is typically utilized to model viscoelastic materials. Each parallel unit composed of a serially connected spring and a damper is called a Maxwell arm.

where  $x$  is the displacement applied to the arm ( $\dot{x}$  represents its time derivative);  $F$  is the force applied to the arm,  $\dot{F}$  is the time derivative of the force; and  $k_1$  and  $b_1$  are the stiffness and damping coefficients of the spring and the damper, respectively.

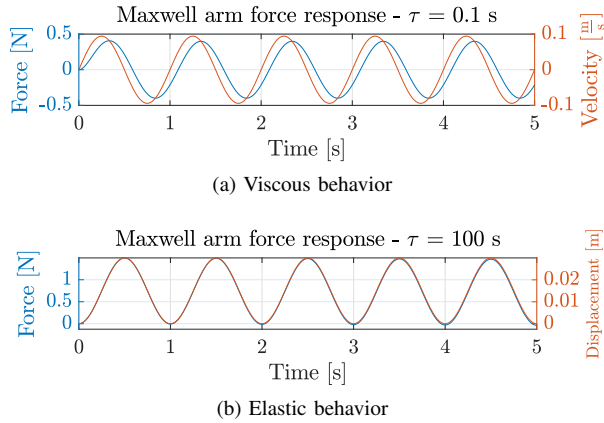


Fig. 4. Force response of a Maxwell arm with (a) small and (b) large time constants.

We can transform (3) into Laplace domain and re-arrange it to obtain the transfer function between the displacement  $X(s)$  and force  $F(s)$ :

$$\frac{F(s)}{X(s)} = \frac{\tau k_1 s}{\tau s + 1} \quad (4)$$

where  $\tau = b_1/k_1$ .

#### A. Limit Cases

If we look at the transfer function in (4) when  $\tau \rightarrow 0$ :

$$\lim_{\tau \rightarrow 0} F(s) = \lim_{\tau \rightarrow 0} \frac{\tau k_1 s}{\tau s + 1} X(s) = \lim_{\tau \rightarrow 0} \frac{\frac{b_1}{k_1} k_1 s}{\tau s + 1} X(s) = b_1 s X(s), \quad (5)$$

we can see that a Maxwell arm behaves like a damper (see Fig. 4a).

On the other hand, when  $\tau \rightarrow \infty$ , the response of a Maxwell arm is equivalent to that of a spring (see (6) and Fig. 4b).

$$\begin{aligned} \lim_{\tau \rightarrow \infty} F(s) &= \lim_{\tau \rightarrow \infty} \frac{\tau k_1 s}{\tau s + 1} X(s) \\ &= \lim_{\tau \rightarrow \infty} \frac{k_1 s}{s + \frac{1}{\tau}} X(s) \\ &= k_1 X(s) \end{aligned} \quad (6)$$

#### B. Harmonic Response of a Maxwell Arm

To look at the harmonic response of a Maxwell arm, we can plug-in  $j\omega$  for  $s$  in the transfer function given in (4) to obtain the complex stiffness as

$$k_C(\omega) = \frac{\tau k_1 j \omega}{1 + \tau j \omega}, \quad (7)$$

$$k_C(\omega) = \underbrace{\frac{k_1 \omega^2 \tau^2}{\omega^2 \tau^2 + 1}}_{k_S} + j \underbrace{\frac{k_1 \omega \tau}{\omega^2 \tau^2 + 1}}_{k_L}. \quad (8)$$

The above formulation of complex stiffness is similar to the one given in (1), and can be alternatively written in phasor notation as

$$k_C(\omega) = |k_C| \angle \phi \quad (9)$$

where  $\phi = \tan^{-1}(k_L/k_S) = \tan^{-1}(1/\omega\tau)$ , and the magnitude  $|k_C| = \sqrt{k_S^2 + k_L^2}$ . In Fig. 5, a contour plot of the phase angle for a range of frequency  $f$  ( $\omega/(2\pi)$ ) and time constant  $\tau$  pairs is shown. The yellow regions below the black curve correspond to a more damper-like behavior while the red regions above the blue curve correspond to a more spring-like behavior. The behavior in the orange region (in between the black and blue curves) is neither damper nor spring-like.

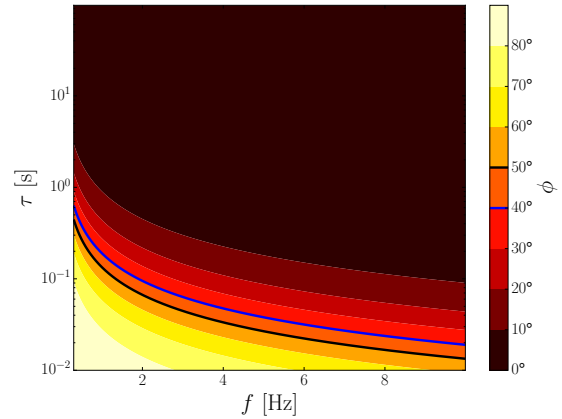


Fig. 5. Contour plot of the phase angle  $\phi$  with respect to the time constant  $\tau$  in log scale and frequency  $f$  in linear scale. The behavior is damper-like in regions under the black curve (shades of yellow), spring-like in regions above the blue curve (shades of red), and neither damper nor spring-like in the region between the black and blue curves (orange colored region).

Within the frequency range of human hand motion (0 to 10 Hz), mechanical behavior of a Maxwell arm is governed by its time constant and the stimulation frequency. The effect of time constant becomes more dominant as the frequency

is increased (see the decreasing slope of the contours as the frequency grows in Fig. 5). For this reason, we investigate haptic perception of viscoelastic materials in the form of a Maxwell arm at low frequencies of hand motion ( $f = 0.5$  and  $1$  Hz) for both small and large values of the time constant.

### III. EXPERIMENT 1: PERCEIVED COMPLEX STIFFNESS OF MAXWELL ARM

In all of our experiments, we assumed that people tend to make sinusoidal hand movements while exploring viscoelastic materials. So, we have considered only the dynamic loading conditions. As shown earlier, under dynamic loading, the steady-state response of viscoelastic materials differs from basic linear materials such as spring and damper only in the phase. In our experiments, we compared the perceived force magnitude of a Maxwell arm's with that of a damper (spring) for a small (large) value of  $\tau$  (see Table II) to determine the point of subjective equality. The  $\tau$  values for the reference stimuli are chosen such that transient dies out very quickly (for small  $\tau$ ), or persists during the interaction (for large  $\tau$ ) (see Fig. 4).

#### A. Participants

Nine healthy participants (1 female and 8 males with an average age of  $27.9 \pm 3.2$  years old) performed the experiments and only one participant is left-handed. The study was approved by the Koc University Human Ethics Committee and the participants gave their signed consent.

#### B. Apparatus

Visual and haptic representations of the stimuli were rendered using a computer screen and a Phantom Premium 1.0 device with the thimble-gimbal attached, respectively. An orthogonal transformation was used between the reference frames of graphical scene and haptic device. Also, to eliminate possible perspective effects, orthographic projection was used for displaying the graphics on the screen.

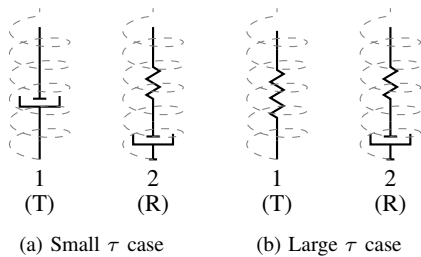


Fig. 6. Stimulus pairs in Experiment 1. Dashed helices are the visual representations of the stimuli, whereas units drawn with solid lines show the underlying mechanical behavior. The letters “R” and “T” denote the reference stimuli rendered as a Maxwell arm and the test stimuli, respectively.

#### C. Stimuli

The graphical representation of all stimuli consisted of a yellow-colored plate (a surface that the blue-colored haptic cursor makes a contact) and a cyan-colored helical spring under the plate (see Fig. 7). When the participant compressed a Maxwell arm, the force response of the Maxwell arm was

TABLE II  
PARAMETERS OF REFERENCE STIMULI

	Small $\tau$		Large $\tau$	
$f$	1 Hz	0.5 Hz	1 Hz	0.5 Hz
$\tau$	0.1 s	0.1 s	100 s	100 s
$k_1$	50 N/m	50 N/m	50 N/m	50 N/m
$b_1$	5 N s/m	5 N s/m	5000 N s/m	5000 N s/m
$ k_C $	0.0266	0.0150	0.0500	0.0500
$k_S$	0.0142	0.0045	0.0500	0.0500
$k_L$	0.0225	0.0143	$7.9577e-5$	$1.5915e-4$
$\phi$	$57.8581^\circ$	$72.5594^\circ$	$0.0912^\circ$	$0.1824^\circ$
$\delta t$	-89.2831 s	-96.8922 s	1.0132 s	0.2533 s

computed in real-time by discretizing (3) as in [27] and then displayed to the participant in the direction normal to the surface of the plate.

#### D. Procedure

We conducted a one-up/one-down adaptive staircase procedure using a two-interval two-alternative forced-choice (2I-2AFC) paradigm. There were four sessions ( $2\tau \times 2f$ ) which were conducted in a randomized order. In each session of the experiment, the participants were presented with two types of virtual stimuli: a reference stimulus which is a Maxwell arm with a set of fixed parameters, and a test stimulus which is a damper if the time constant of the Maxwell arm was  $\tau = 0.1$  s or a spring if  $\tau = 100$  s (see Fig. 6). The task was to determine the more viscous (stiffer) stimulus when the time constant was small (large). The parameters of the reference stimuli and their values are given in Table II. The parameter values corresponding to the boldface letters were set by us while the rest of the values were calculated by the model.

For both small and large values of  $\tau$ , the perceived magnitude of the complex stiffness of a Maxwell arm, i.e. the subjectively equal damping coefficient or stiffness value, was estimated by a separate psychophysical experiment. In each trial, the order of the reference and test stimuli were randomized while the same order was displayed to all participants. At the start of each experiment, a considerably high value of complex stiffness ( $b_{\text{test}}$  or  $k_{\text{test}}$  depending on the value of  $\tau$ ) was chosen for the test stimulus. If the test stimulus was judged to have a higher complex stiffness than that of the reference then its complex stiffness was logarithmically decreased, and vice versa.

Before each session, the participants were asked to sit in front of a computer screen and put their forearms on an adjustable arm rest. They put the index finger of their dominant hand inside the thimble of the haptic device. To avoid slippage, they were instructed to support the thimble with their thumb in a precision grip pose. The haptic interface point was displayed by a blue cursor on the screen.

While exploring the stimuli, the participants were required to follow the procedure depicted in Fig. 7. First, they were asked to touch the red-colored snap line (Fig. 7a) to constrain their movement in the normal direction. A light guiding force

was applied to bring them back to the snap line when their finger deviated from it. Then, they were asked to touch the red colored cursor on the surface of the plate, whose color turned to yellow upon contact (Fig. 7b) and then to green after 0.5 ms (Fig. 7c) to signal that the trial is ready to go. Finally, they were asked to follow the magenta-colored reference cursor, which appears on the screen once the pre-set threshold velocity was exceeded by the participant (Fig. 7d). The trajectory of the reference cursor was a sinusoid with a frequency  $f = 0.5$  and 1 Hz. In each trial, the stimulus to be explored was always displayed in the middle of the screen. Participants were allowed to explore each stimulus for 3 s only. After this duration, the next stimulus in the queue came sliding into the middle of the screen and the same exploration procedure was repeated. After both stimuli were explored, the participants responded to the question of which one of the two stimuli was more viscous (stiffer) for the case of small (large) time constant. The participants were allowed to repeat the same trial only once more if they were undecided after the first exploration.

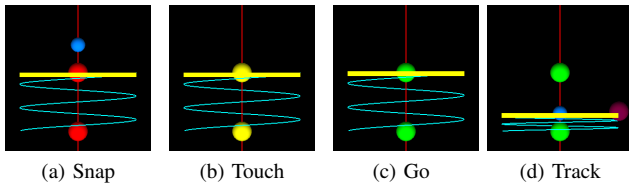


Fig. 7. Procedural steps of the experiments

### E. Data Analysis

In the first five reversals, the step size used in our staircase method was large. In the remaining seven reversals, it was small. To find the PSE for the complex stiffness magnitude of a Maxwell arm with respect to that of a the test stimulus (damper or spring), the mean value of the last six reversals were considered. An example experiment session is depicted in Fig. 8.

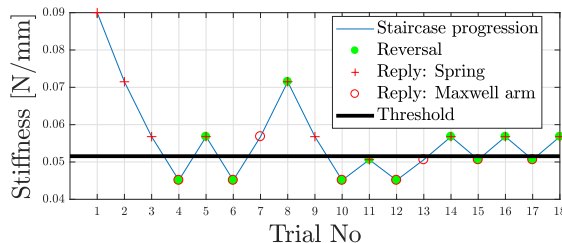


Fig. 8. An example run of the adaptive staircase.

### F. Results

The PSE results of the first set of experiments are normalized by the complex stiffness of the reference stimuli (See Table II for the reference  $k_C$  values) and are depicted in Fig. 9.

To investigate whether the frequency of stimulation and/or the time constant affect the perceived magnitude of stiffness or viscosity, a two-way repeated measures ANOVA was performed. No significant effect of frequency was observed ( $F(1, 8) = 0.109$ ,  $p = 0.75$ ). However, the effect of time constant was found to be significant ( $F(1, 8) = 24.378$ ,  $p = 0.0011$ ). There was no interaction between the frequency and the time constant ( $F(1, 8) = 0.941$ ,  $p = 0.361$ ).

As explained in Section II, the force response magnitude of a Maxwell arm depends on its complex stiffness. For each time constant ( $\tau = 0.1$  and 100 s), one sample t-tests were performed to compare the resulting PSE values with the magnitude of complex stiffness. Significant differences were found for small values of  $\tau$  ( $p < 0.001$ ,  $t = -7.48$ ), whereas no such effect was observed when  $\tau$  is large ( $p = 0.063$ ,  $t = -2.00$ ).

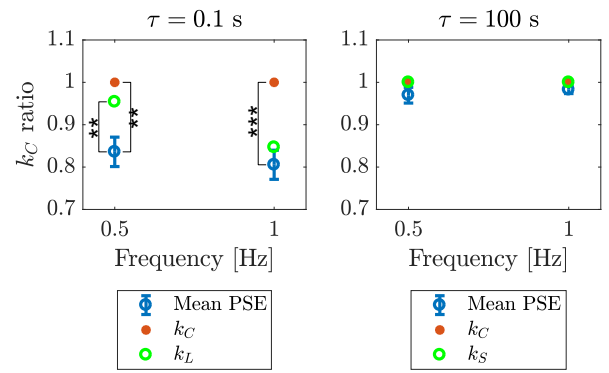


Fig. 9. Mean PSE results for magnitudes. The error bars represent the standard error of the mean.

For the small time constant, another set of one sample t-tests were performed for testing the null hypothesis that PSE values were equal to  $k_L$ , the imaginary (dissipative) component of the complex stiffness. No significant difference was found for  $f = 1$  Hz ( $p = 0.2636$ ,  $t = -1.20$ ), though the difference was significant for  $f = 0.5$  Hz ( $p = 0.0093$ ,  $t = -3.40$ ).

Similarly, for the large time constant, one sample t-tests were performed again for testing the null hypothesis that PSE values were equal to  $k_S$ , the real (storage) component of the complex stiffness. For both stimulation frequencies, no significant difference was found ( $p = 0.1414$ ,  $t = -1.63$  for 0.5 Hz, and  $p = 0.0955$ ,  $t = -1.89$  for 1 Hz). Note that values of  $k_L$  and  $k_S$  are different for different stimulation frequencies, hence separate t-tests were performed for different stimulation frequencies.

## IV. EXPERIMENT 2: DISCRIMINATION OF MAXWELL ARM FROM BASIC LINEAR MATERIALS

In the second experiment, we searched for the upper and lower bounds of the phase angle that makes a Maxwell arm subjectively equal to a damper ( $\phi = 90^\circ$ ) and a spring ( $\phi = 0^\circ$ ), respectively. Again, the same participants were recruited, and the apparatus, stimuli, most of the experimental

procedure, and data analysis methods were kept the same as those of the experiments presented in Section III.

We again conducted a one-up/one-down adaptive staircase method, but this time using a three-interval two-alternative forced-choice (3I-2AFC) paradigm. The participants were asked to determine the stimulus that was different from the reference stimulus presented in the second interval. This reference stimulus was a damper (spring) when the upper (lower) bound for the phase angle was investigated. Also, either the first or third interval was randomly assigned to contain a stimulus that was identical to the reference stimulus presented in the second interval. Lastly, the test stimulus (a Maxwell arm whose time constant was altered according to the adaptive procedure) was placed at the remaining interval (see Fig. 10).

#### A. Procedures

For the upper (lower) bound, the damping (stiffness) coefficient of the reference stimulus and the dissipative (storage) component of the test stimulus were set to be equal based on the results of the first set of experiments. At the beginning of the experiment, the initial phase angle was chosen to be far from the phase angle the reference stimulus ( $90^\circ$  for damper and  $0^\circ$  for spring) so that discriminating the Maxwell arm from a damper (or a spring) was easy. Every time the participant provided a correct response, the phase angle of the test stimulus was increased (decreased) when the damper (spring) was the reference stimulus, and vice versa.

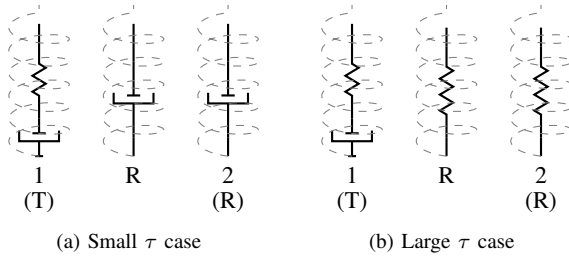


Fig. 10. Stimulus triplets in Experiment 2. Dashed helices are the visual representations of the stimuli, whereas units drawn with solid lines show underlying mechanical behavior. The letters “R” and “T” denote the reference stimuli and the test stimuli, respectively.

#### B. Results

The PSE values of the phase angle with respect to  $0^\circ$  and  $90^\circ$  were found by averaging the last six reversals of the staircase method.

A repeated measures ANOVA was performed on the mean PSE outcomes with two within subjects variables: stimulation frequency and time constant. For the effect of stimulation frequency, no significant differences were observed ( $F(1, 8) = 0.007$ ,  $p = 0.934$ ). However, significant differences were found for the time constant ( $F(1, 8) = 11.765$ ,  $p = 0.014$ ). No interaction was observed between the frequency and time constant ( $F(1, 8) = 0.384$ ,  $p = 0.558$ ).

The distance between the perceptual upper bound and  $90^\circ$  (damper), and between the perceptual lower bound and  $0^\circ$  (spring) were compared using one sample t-tests and found

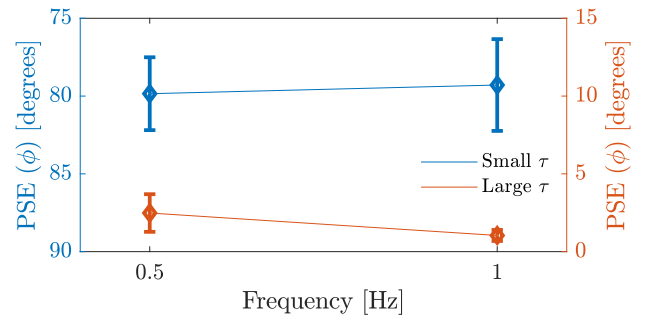


Fig. 11. Mean PSE results for the phase angle with respect to boundaries. The error bars represent the standard error of the mean.

to be significant ( $p < 0.001$  for the upper bound;  $p = 0.013$  for the lower bound).

#### V. DISCUSSION

In this study, we first conducted 2I-2AFC staircase experiments to investigate how the perceived magnitude of complex stiffness changes in a Maxwell arm for small and large  $\tau$  values. For small  $\tau$ , the magnitude of the complex stiffness was underestimated. Note that the test stimulus for small  $\tau$  was a damper, whose force response shows a phase lag of  $90^\circ$  with respect to the displacement input under dynamic loading, whereas a Maxwell arm shows a smaller phase lag than  $90^\circ$  (see Table II). The relatively smaller phase lag of a Maxwell arm might be viewed as a phase lead in comparison to that of the damper. Similarly, in [11], the authors also observed that the perceived stiffness of a spring was lower (higher) when there was a phase lead (lag) between force response and displacement input. However, in the case of a large  $\tau$ , the phase difference was small and no significant underestimation of the complex stiffness magnitude was observed in our experiments.

We then conducted 3I-2AFC experiments to investigate the PSE of a Maxwell arm to basic linear materials as a function of phase angle. Two equivalent dampers (springs) were used as the reference stimuli for estimating the upper (lower) bounds of the phase angle of the Maxwell arm for the chosen stimulation frequencies. The distance between the PSE values estimated for the upper bound of the phase angle to its actual limit ( $90^\circ$ ) was significantly higher than those of the lower bound when  $f = 0.5$  and 1 Hz. For example, our results show that if the phase angle is below  $2.5^\circ$  (or above  $79.8^\circ$ ) when  $f = 0.5$  Hz, then a Maxwell arm was perceptually equivalent to a spring (damper). This suggests that a Maxwell arm with a large time constant can be more easily discriminated from a spring than a Maxwell arm with a small time constant can be discriminated from a damper. The exponentially decaying transient of the response could be the reason of this difference. For a Maxwell arm with small time constant, the transient of the response has a small magnitude and disappears very quickly, whereas for a Maxwell arm with large time constant, the exponential decay of the transient is small for a short duration of stimulation, but still it might have been used as a cue by the participants.

## VI. CONCLUSIONS

In this study, we proposed a new approach for the psychophysical investigation of human perception of viscoelasticity. This is a complex problem since the viscoelastic materials show a time and history dependent behavior, and are neither purely elastic nor purely viscous. By using the concept of complex stiffness  $k_C(\omega)$ , we first represented the force response of a Maxwell arm using its magnitude and phase angle. The Maxwell arm is the basic unit of GMM that is typically used in modeling viscoelastic materials. We then compared the perceived force response of a Maxwell arm with those of basic linear material models: a damper and a spring. They represent the limits cases of a Maxwell arm. In our future studies, we plan to obtain a full psychometric curve for a Maxwell arm by varying its time constant under different stimulation frequencies. Additionally, we will extend the scope of the work from a single Maxwell arm to a GMM. Although the behavior of a GMM is more complex than that of a single Maxwell arm, the concept of complex stiffness can be generalized to GMM by linearly adding the complex stiffness contribution of each arm in the frequency domain to reduce the complexity of psychophysical investigations.

## ACKNOWLEDGMENT

The authors thank Dr. Wouter M. Bergmann Tiest for his comments and feedback at the very initial phase of this work; and Ahmet Guzererler, Omer Sirin, Utku Erdem, Yasemin Vardar, and all other members of the Robotics and Mechatronics Lab at Koc University for their time in participating the experiments and providing valuable feedback.

## REFERENCES

- [1] L. L. Nicholson, R. D. Adams, and C. G. Maher, "Manual discrimination capability when only viscosity is varied in viscoelastic stiffness stimuli," *Journal of Manipulative and Physiological Therapeutics*, vol. 26, no. 6, pp. 365–373, 2003.
- [2] G. Tabilo-Munizaga and G. V. Barbosa-Cánovas, "Rheology for the food industry," *Journal of Food Engineering*, vol. 67, no. 1, 2005.
- [3] N. I. Durlach, L. A. Delhorne, A. Wong, W. Y. Ko, W. M. Rabinowitz, and J. Hollerbach, "Manual discrimination and identification of length by the finger-span method," *Perception & Psychophysics*, vol. 46, no. 1, pp. 29–38, 1989.
- [4] R. P. Erickson, "Parallel "population" neural coding in feature extraction," *The neurosciences: Third study program*, pp. 155–169, 1974.
- [5] X. D. Pang, H. Z. Tan, and N. I. Durlach, "Manual discrimination of force using active finger motion," *Perception & Psychophysics*, vol. 49, no. 6, pp. 531–540, 1991.
- [6] L. A. Jones, "Matching forces: constant errors and differential thresholds," *Perception*, vol. 18, no. 5, pp. 681–687, 1989.
- [7] H. Z. Tan, X. D. Pang, and N. I. Durlach, "Manual resolution of length, force, and compliance," *Advances in Robotics*, vol. 42, pp. 13–18, 1992.
- [8] L. A. Jones and I. W. Hunter, "A perceptual analysis of stiffness," *Experimental Brain Research*, vol. 79, no. 1, pp. 150–156, 1990.
- [9] G. L. Beauregard, M. A. Srinivasan, and N. I. Durlach, "The manual resolution of viscosity and mass," in *Proceedings of the ASME Dynamic Systems and Control Division*, vol. 57, no. 2, 1995.
- [10] L. A. Jones and I. W. Hunter, "A perceptual analysis of viscosity," *Experimental Brain Research*, vol. 94, no. 2, pp. 343–351, 1993.
- [11] A. Pressman, A. Karniel, and F. A. Mussa-Ivaldi, "Perception of Delayed Stiffness," in *The First IEEE/RAS-EMBS International Conference on Biomedical Robotics and Biomechanics, 2006. BioRob 2006*, Feb 2006, pp. 905–910.
- [12] A. Pressman, L. J. Welty, A. Karniel, and F. A. Mussa-Ivaldi, "Perception of Delayed Stiffness," *The International Journal of Robotics Research*, vol. 26, no. 11-12, pp. 1191–1203, 2007.
- [13] M. Rank, Z. Shi, H. J. Müller, and S. Hirche, *The Influence of Different Haptic Environments on Time Delay Discrimination in Force Feedback*. Springer Berlin Heidelberg, 2010, pp. 205–212.
- [14] R. H. LaMotte, "Softness Discrimination With a Tool," *Journal of Neurophysiology*, vol. 83, no. 4, pp. 1777–1786, 2000.
- [15] U. Kocak, K. L. Palmerius, C. Forsell, A. Ynnerman, and M. Cooper, "Analysis of the JND of Stiffness in Three Modes of Comparison," in *Haptic and Audio Interaction Design: 6th International Workshop, HAID 2011, Kusatsu, Japan, August 25-26, 2011. Proceedings*, E. W. Cooper, V. V. Kryssanov, H. Ogawa, and S. Brewster, Eds. Springer Berlin Heidelberg, 2011, pp. 22–31.
- [16] E. Fakhoury, P. Culmer, and B. Henson, "The Effect of Vision on Discrimination of Compliance Using a Tool," *International Journal of Human-Computer Interaction*, vol. 30, no. 11, pp. 882 – 890, 2014.
- [17] W. M. B. Tiest, A. C. L. Vrijling, and A. M. L. Kappers, "Haptic Discrimination and Matching of Viscosity," *IEEE Transactions on Haptics*, vol. 6, no. 1, pp. 24–34, 2013.
- [18] W. M. B. Tiest and A. M. L. Kappers, "Cues for Haptic Perception of Compliance," *IEEE Transactions on Haptics*, vol. 2, no. 4, pp. 189–199, Oct 2009.
- [19] M. Rank, T. Schauf, A. Peer, S. Hirche, and R. L. Klatzky, "Masking Effects for Damping JND." in *Proceedings of EuroHaptics*, ser. Lecture Notes in Computer Science, P. Isokoski and J. Springare, Eds., vol. 7283. Springer, 2012, pp. 145–150.
- [20] F. Barbagli, K. Salisbury, C. Ho, C. Spence, and H. Z. Tan, "Haptic Discrimination of Force Direction and the Influence of Visual Information," *CM Transactions on Applied Perception*, vol. 3, no. 2, pp. 125–135, Apr. 2006.
- [21] E. Samur, M. Sedef, C. Basdogan, L. Avtan, and O. Duzgun, "A robotic indenter for minimally invasive measurement and characterization of soft tissue response," *Medical Image Analysis*, vol. 11, no. 4, pp. 361–373, 2007.
- [22] B. Yarpuzlu, M. Ayyildiz, O. E. Tok, R. G. Aktas, and C. Basdogan, "Correlation between the mechanical and histological properties of liver tissue," *Journal of the Mechanical Behavior of Biomedical Materials*, vol. 29 Supplement C, pp. 403–416, 2014.
- [23] C. Gokgol, C. Basdogan, and D. Canadinc, "Estimation of fracture toughness of liver tissue: Experiments and validation," *Medical Engineering & Physics*, vol. 34, no. 7, pp. 882–891, 2012.
- [24] S. Ocal, M. U. Ozcan, I. Basdogan, and C. Basdogan, "Effect of preservation period on the viscoelastic material properties of soft tissues with implications for liver transplantation," *Journal of Biomechanical Engineering*, vol. 132, no. 10, p. 101007, 2010.
- [25] A. Pressman, I. Nisky, A. Karniel, and F. A. Mussa-Ivaldi, "Probing Virtual Boundaries and the Perception of Delayed Stiffness," *Advanced Robotics*, vol. 22, no. 1, pp. 119–140, 2008.
- [26] I. Nisky, A. Pressman, C. M. Pugh, F. A. Mussa-Ivaldi, and A. Karniel, "Perception and Action in Teleoperated Needle Insertion," *IEEE Transactions on Haptics*, vol. 4, no. 3, pp. 155–166, July 2011.
- [27] B. B. Baran and C. Basdogan, "Force-Based Calibration of a Particle System for Realistic Simulation of Nonlinear and Viscoelastic Soft Tissue Behavior," in *Proceedings of EuroHaptics*, ser. Lecture Notes in Computer Science. Springer Berlin Heidelberg, July 2010, pp. 23–28.